BULLETIN OF THE EARTHQUAKE
RESEARCH INSTITUTE
Vol. 41 (1963), pp. 217-241

14. Crustal Structure in Japan from the Phase Velocity of Rayleigh Waves.

Part 2. Rayleigh Waves from the Aleutian Shock of March 9, 1957.

By Katsutada KAMINUMA,
Graduate School, The University of Tokyo,
and
Keiiti AKI,
Earthquake Research Institute.

(Read Oct. 23, 1962.—Received Dec. 28, 1962.)

1. Introduction

The phase velocity of Rayleigh waves were utilized in a study of the crustal structure in Japan by Aki (1961). In order to extend the area covered by the phase velocity measurement and to confirm the conclusions obtained in the first paper, we studied the records of the Aleutian shock of March 9, 1957 (14h 22m 27s G.M.T., 51°N 175°W, M: 8–8 1/2) in the present paper. The direction of approach was nearly at right angles to the trend of Japanese Islands for the waves studied in the first paper, but parallel for the waves studied in the present paper.

The records were kindly supplied from the seismological stations operated by the Japan Meteorological Agency. Rayleigh waves with periods 20 to 40 sec from this earthquake are very clearly recorded by Wiechert seismographs at many of the J. M. A. stations. The Wiechert seismographs operated at these stations are adjusted to maintain uniform charactristic (pendulum period 5.0 sec, geometric magnification 70 to 80 and the damping ratio 6 to 8). The dynamic magnification of this instrument at the periods 30 sec is about 1.5 and the trace amplitudes of Rayleigh waves from the shock were 2 to 6 cm on the records.

In this paper we were able to include those areas which were not covered in the first paper, such as southern Hokkaido, Hokuriku, Kii and other regions. From both studies, we determined the crustal thickness nearly everywhere in the Japanese Islands except northern Hokkaido by the phase velocity method of Rayleigh waves.

In western Japan the value of phase velocity obtained in the present paper agrees with the value in the first paper, but in central Japan (Kanto and Chubu) there is a small disagreement. It may be that the phase velocity depends on the direction of approach in the latter regions.

2. Data

The records of Wichert seismographs were supplied from 51 J. M. A. stations. However, 6 of them were not used in the analysis, because

Table 1. List of Stations.

Station	Abbreviation	Latitude		Longitude	
		deg.	min.	deg.	min.
Nemuro	N E	43	19.7	145	35.4
Sapporo	S A	43	03.5	141	19.9
Mori	M R	42	06.3	140	34.5
Obihiro	O B	42	55.3	143	13.2
Muroran	M U	42	19.7	140	58.0
Aomori	A O	40	51.0	140	42.1
Morioka	M O	39	41.7	141	10.2
Miyako	M Y	39	38.7	141	58.1
Sendai	S E	38	15.6	140	54.0
Fukushima	F U	37	45.3	140	28.5
Onahama	O N	36	56.7	140	54.3
Kakioka	K K	36	13.9	140	11.6
Kumagaya	K U	36	08.8	139	23.0
Tokyo	T K	35	41.3	139	45.8
Yokohama	Y O	35	26.2	139	39.4
Choshi	C H	35	43.5	140	50.6
Tomisaki	T S	34	55.1	139	49.7
Oshima	O S	34	45.7	139	22.8
Aikawa	A I	38	01.2	138	14.5
Wajima	W A	37	23.4	136	53.8
Toyama	T Y	36	42.4	137	12.3
Nagano	N A	36	39.6	138	11.8
Kofu	K F	35	39.9	138	33.5
Mishima	M S	35	06.7	138	55.7
Shizuoka	S Z	34	58.4	138	24.4
Nagoya	N Y	35	09.9	136	58.1
Gifu	G I	35	23.8	136	45.9
Hikone	H K	35	16.4	136	14.8
Kameyama	K A	34	51.3	136	27.9
Owashi	O W	34	03.9	136	11.7
Shionomisaki	S H	33	26.9	135	45.8
Osaka	O K	34	39.0	135	32.2
Toyooka	T U	35	32.1	134	49.3
Kyoto	K Y	35	00.7	135	44.3
Sumoto	S U	34	20.1	134	54.5
Hamada	H A	34	53.6	132	04.4
Hiroshima	H R	34	21.8	132	26.2
Takamatsu	T A	34	19.1	134	03.5
Matsuyama	M A	33	50.4	132	46.8
Kochi	K O	33	33.9	133	33.1
Shimizu	S I	32	46.5	132	57.7
Fukuoka	F K	33	34.7	130	22.8
Kumamoto	K M	32	48.6	130	42.6
Tomie	T M	32	36.5	128	45.9
Miyazaki	M Z	31	55.0	131	25.6

of poor time-keeping or the presence of large microseisms. The list of the 45 stations used in the analysis is given in Table 1.

The instruments of three stations, Obihiro, Muroran and Choshi are the J. M. A. 53 type seismographs. The deviation of instrumental phase

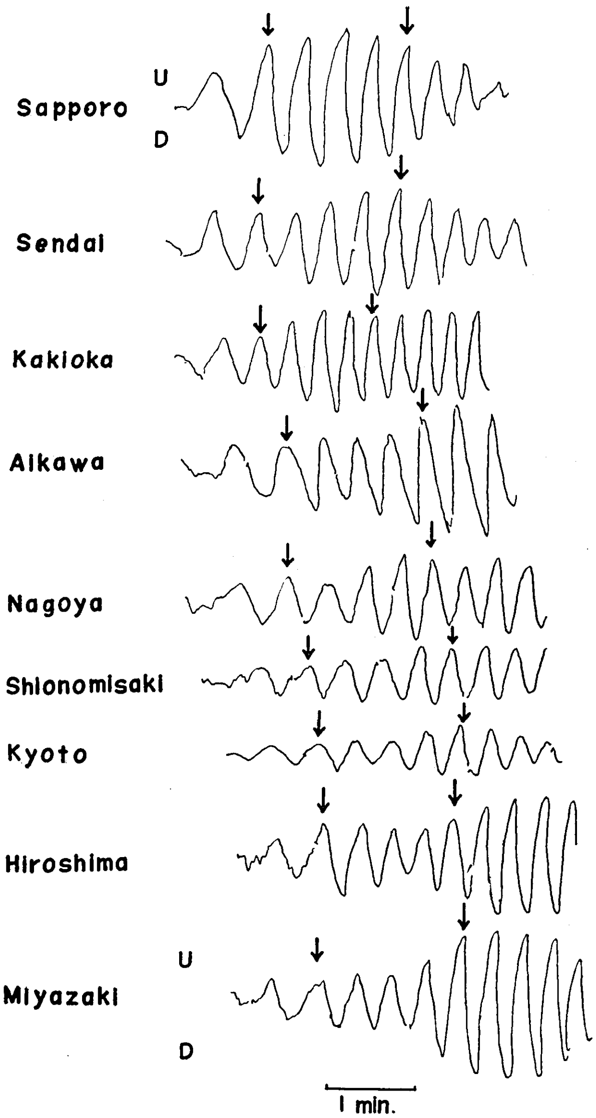

Fig. 1. The vertical component seismograms of Rayleigh waves from the Aleutian shock of March 9, 1957. The arrows indicate the 2nd and the 6th peaks.

delay at these stations from that of the Wiechert seismograph are corrected in the phase velocity measurement.

The records of the Rayleigh waves at various stations in Japan are shown in Fig. 1. It can be seen in this figure that the onset of the Rayleigh waves are clearly identifiable on the records. There was no difficulty in tracing the 1st peak and also the following peaks from station to station. We used only records of vertical component seismograph in the present paper. The arrival times of each peak and trough are determined as follows. Since the amplitudes were very large (the amplitude on the records: 2 to 6 cm), it was difficult to read accurately the arrival times of peaks and troughs. Therefore, we read the arrival times of the zero points of the seismogram traces, that is, we read the

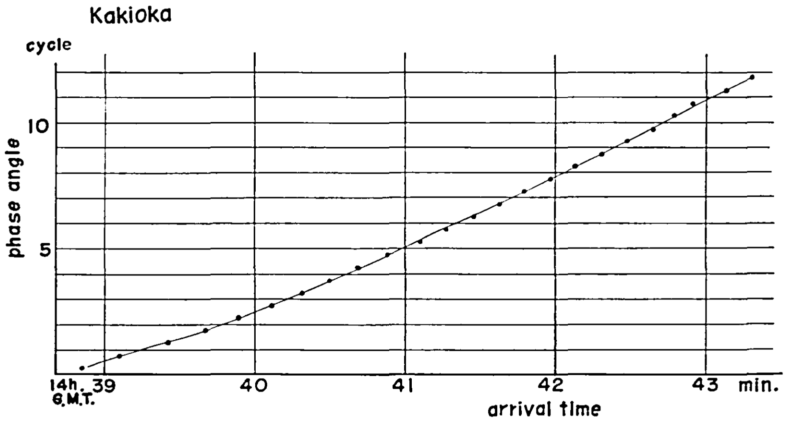

Fig. 2. Arrival times of the phase 1/4 cycle before the peak and the trough at Kakioka. A smooth line was drawn to fit the points, and the times at which the smooth line cuts the ordinate for the peaks 1, 2, 3, 5, and 7 were read off.

times of 1/4 cycle before and after those of the peaks. They are plotted in a figure like that of Fig. 2, where the ordinate is the phase angle measured in cycle.

A smooth line is drawn to coincide with the arrival time points for the station, and times are measured at which the smooth line cuts the ordinate corresponding to each peak.

The periods of the peak are determined from the slope of arrival time curve.

The arrival times are determined for at least 7 peaks at each of the 45 stations. Table 2 lists the arrival times and periods of the 1st, 2nd, 3rd, 5th and 7th peak obtained at these stations.

Table 2. Arrival times and periods at each station.

Station	1st peak			2nd peak			3rd peak			5th peak			7th peak		
	period	arrival time		period	arrival time		period	arrival time		period	arrival time		period	arrival time	
	sec.	min.	sec.	sec.	min.	sec.	sec.	min.	sec.	sec.	min.	sec.	sec.	min.	sec.
Nemuro	38.0	36	01.0	28.0	36	32.5	25.0	36	59.0	24.0	37	47.6	23.0	38	35.2
Sapporo	40.5	37	29.3	32.5	38	06.8	27.5	38	34.0	24.5	39	26.8	22.5	40	11.8
Mori	31.0	38	00.6	28.0	38	26.8	25.0	38	52.3	23.0	39	37.5	19.5	40	19.2
Obihiro				28.5	37	34.5	26.5	37	52.9	23.5	38	41.3	22.0	39	26.3
Muroran				30.0	38	19.0	25.0	38	47.0	24.0	39	35.8			
Aomori	38.5	38	02.5	29.5	38	36.5	28.5	39	05.0	26.5	40	01.5	23.0	40	52.2
Morioka	32.0	38	01.3	27.5	38	31.0	24.0	38	56.1	21.0	39	38.0	21.5	40	22.0
Miyako	34.0	37	53.4	27.0	38	22.8	24.0	38	48.1	22.0	39	33.0	21.0	40	18.8
Sendai	33.5	38	31.0	27.2	39	00.0	24.6	39	24.4	23.0	40	12.9	22.5	40	58.5
Fukushima	34.0	38	47.8	28.0	39	18.6	25.0	39	44.8	23.0	40	31.0	21.5	41	14.4
Onahama	33.5	38	51.9	27.0	39	21.0	24.5	39	46.7	23.0	40	34.3	20.5	41	18.5
Kakioka	34.0	39	15.3	28.0	39	46.0	25.5	40	12.5	23.5	40	58.8	20.5	41	42.4
Kumagaya	35.5	39	33.5	27.5	40	05.2	25.0	40	30.7	24.0	41	20.0	21.0	42	03.8
Tokyo	34.5	39	34.8	28.0	40	04.8	26.0	40	32.8	24.0	41	21.3	21.5	42	04.8
Yokohama	34.5	39	41.0	27.8	40	11.2	25.5	40	38.5	24.0	41	28.3	21.0	42	12.1
Chosi	36.0	39	14.1	28.5	39	46.2	26.0	40	11.4	23.6	41	00.0	21.4	41	43.2
Tomisaki	37.5	39	46.0	28.5	40	20.0	25.5	40	45.9	24.0	41	36.5	21.5	42	22.5
Oshima	35.0	39	57.4	29.0	40	28.8	26.0	40	55.5	24.0	41	45.2	22.0	42	29.5
Aikawa	40.0	39	30.0	31.2	40	05.0	24.5	40	31.0	23.5	41	15.5	23.0	42	01.3
Wajima	35.0	40	06.0	30.5	40	38.6	27.0	41	06.5	23.5	41	53.8	22.0	42	39.0
Toyama	40.0	40	07.3	30.0	40	41.8	26.0	41	09.9	23.0	41	56.5	22.5	42	42.0

(to be continued)

(Table 2. continued)

Station	1st peak			2nd peak			3rd peak			5th peak			7th peak		
	period	arrival time		period	arrival time		period	arrival time		period	arrival time		period	arrival time	
	sec.	min.	sec.	sec.	min.	sec.	sec.	min.	sec.	sec.	min.	sec.	sec.	min.	sec.
Nagano	44.0	39	48.0	29.5	40	24.2	25.5	40	49.5	24.5	41	37.7	22.3	42	25.8
Kofu	35.0	39	58.0	30.0	40	29.6	27.0	40	57.4	23.8	41	45.9	21.7	42	29.0
Mishima	36.5	39	59.5	30.1	40	32.3	27.0	41	00.3	24.0	41	49.5	22.0	42	34.3
Shizuoka	43.0	40	07.5	31.0	40	47.0	26.5	41	13.7	24.5	42	02.3	22.0	42	45.5
Nagoya	42.5	40	38.3	30.0	41	13.3	27.0	41	40.7	24.0	42	29.5	21.5	43	13.9
Gifu	38.0	40	37.0	30.0	41	09.4	25.0	41	37.0	22.8	42	23.3	20.5	43	06.2
Hikone	36.0	40	54.7	29.0	41	27.3	24.9	41	53.8	24.0	42	43.7	21.5	43	28.0
Kameyama	35.5	40	55.0	30.8	41	28.7	28.0	41	57.4	24.5	42	47.4	20.5	43	32.0
Owashi	44.5	41	11.2	31.4	41	49.4	26.5	42	16.8	25.3	43	05.5	21.5	43	51.5
Shionomisaki	36.0	41	33.5	29.0	42	06.0	26.0	42	31.8	24.0	43	25.2	22.3	44	09.4
Osaka	41.0	41	15.5	31.7	41	51.0	27.3	42	19.5	24.0	43	09.0	22.5	43	55.0
Toyooka	41.5	41	13.7	33.5	41	52.5	27.0	42	21.8	24.5	43	09.0	22.7	43	56.0
Kyoto	39.0	41	04.5	31.5	41	40.0	27.0	42	08.3	24.5	42	57.9	22.0	43	44.4
Sumoto	43.0	41	32.4	32.5	42	10.3	26.5	42	38.0	24.0	43	25.9	23.0	44	13.4
Hamada	38.5	42	19.5	32.2	42	56.0	29.8	43	26.0	28.5	44	26.0	24.5	45	19.5
Hiroshima	42.2	42	21.0	34.0	42	58.5	29.0	43	28.8	24.5	44	18.5	22.8	45	05.2
Takamatsu	41.0	41	54.3	29.5	42	26.5	26.2	42	51.4	24.4	43	46.2	23.5	44	32.5
Matsuyama	44.0	42	21.0	31.5	43	02.0	26.0	43	30.0	24.2	44	18.5	22.8	45	04.4
Kochi	37.6	42	17.5	31.5	42	49.6	27.0	43	18.0	24.8	44	07.6	24.5	44	56.9
Shimizu	37.5	42	41.5	31.5	43	15.5	26.8	43	43.2	25.0	44	33.3	23.2	45	20.1
Fukuoka	41.0	43	12.0	33.0	43	50.0	28.5	44	21.2	24.6	45	14.3	23.3	46	00.5
Kumamoto	47.5	43	16.8	33.0	43	59.5	27.2	44	29.3	23.8	45	20.1	22.5	46	06.2
Tomie	37.0	44	41.5	35.0	44	41.5	27.5	45	11.9	23.5	46	28.4	22.5	47	14.0
Miyazaki	41.5	43	26.3	34.2	44	02.5	28.8	44	32.0	25.2	45	25.0	23.6	46	14.0

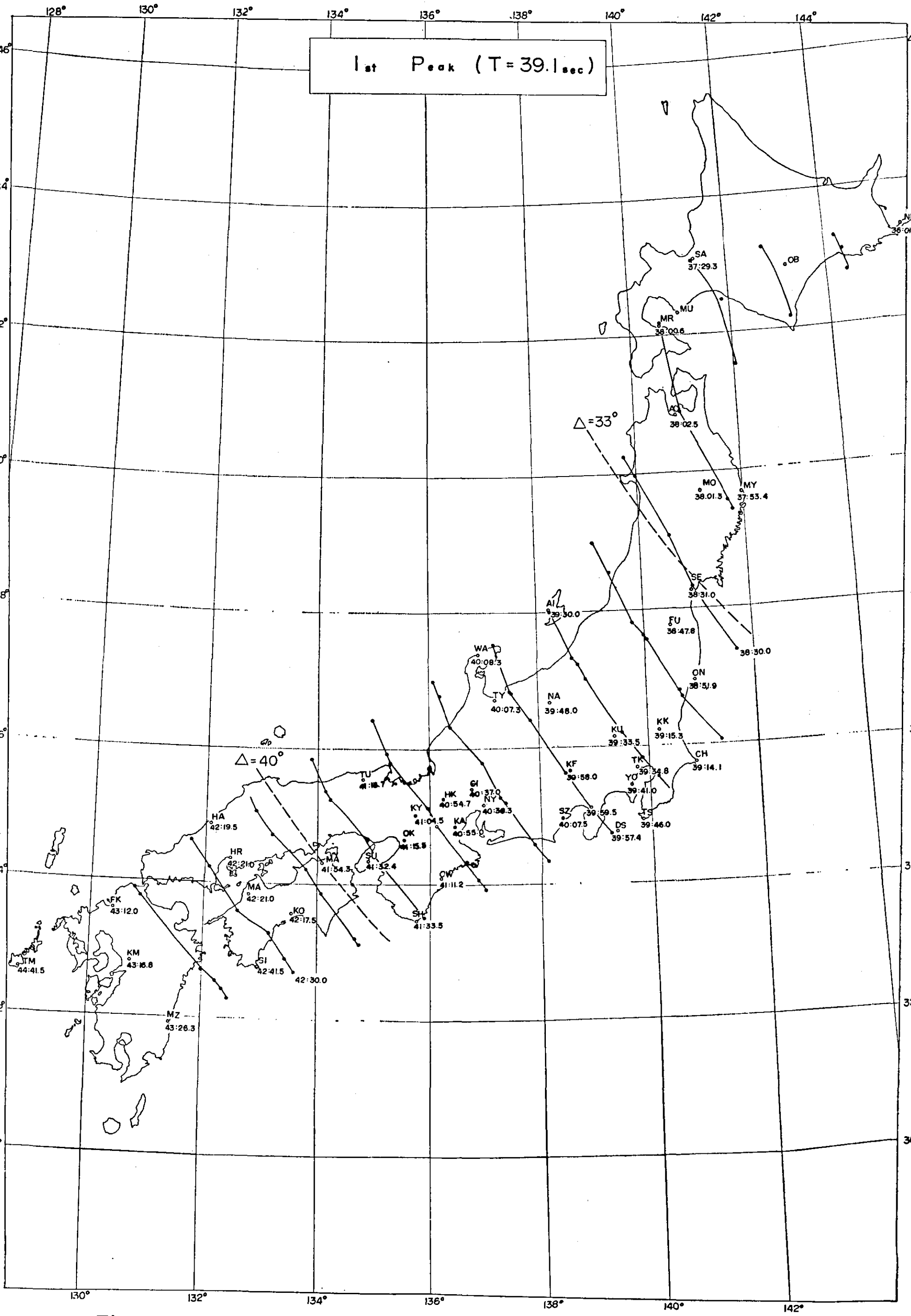

Fig. 3. Wave front of the 1st peak at every 30 seconds across Japan. The broken line indicates the epicentral distance of 33° and 40°.

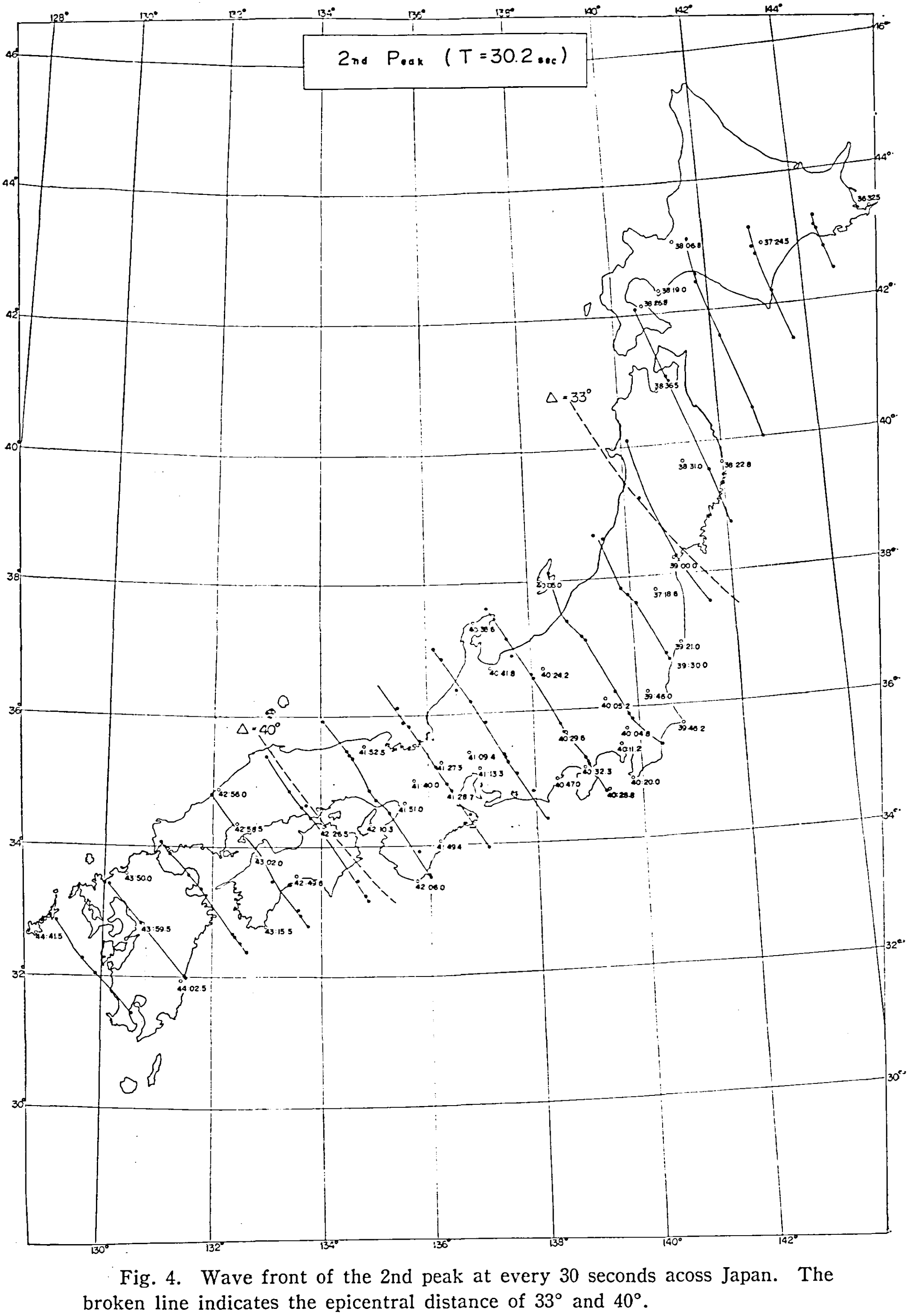

Fig. 4. Wave front of the 2nd peak at every 30 seconds acoss Japan. The broken line indicates the epicentral distance of 33° and 40°.

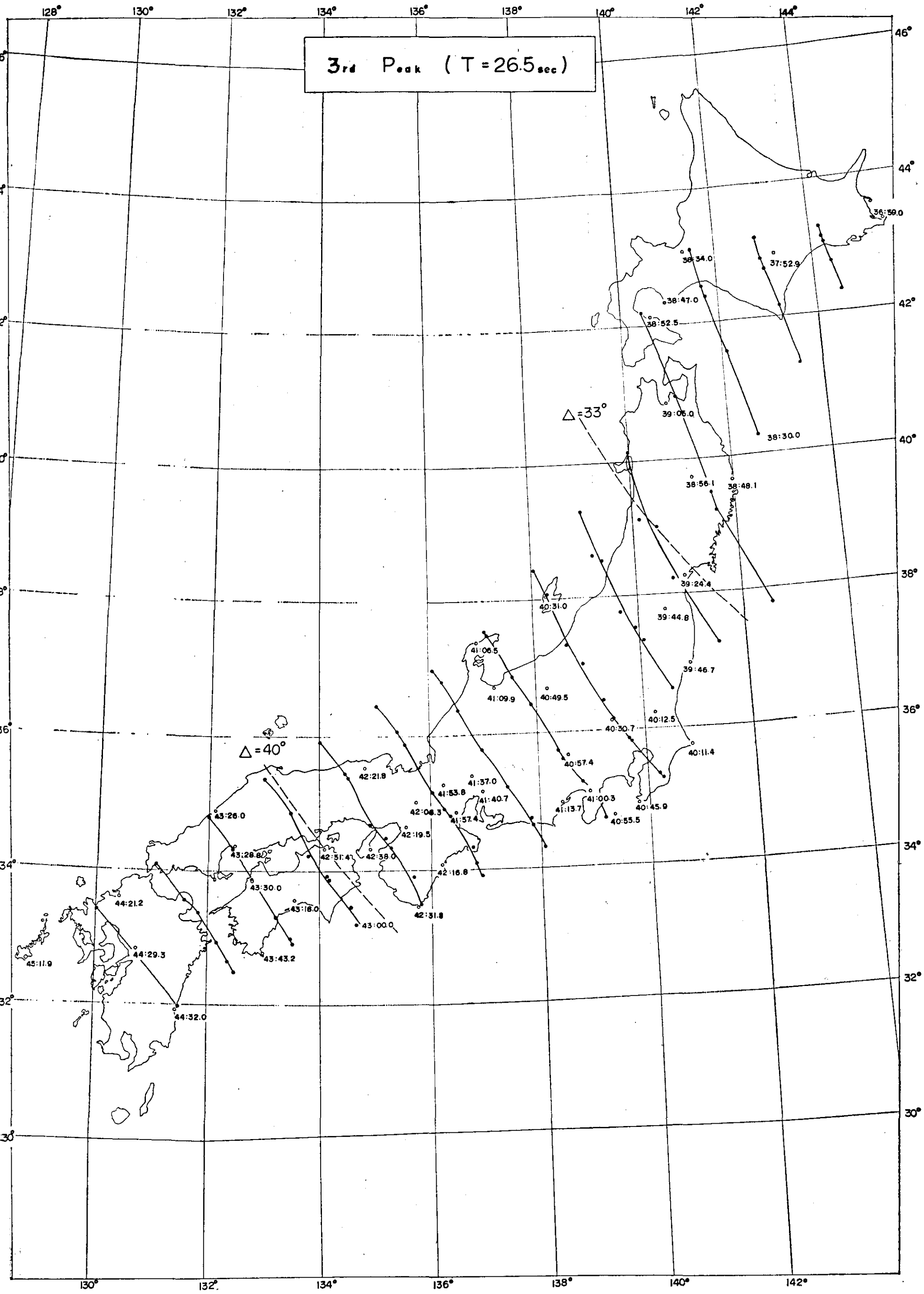

Fig. 5. Wave front of the 3rd peak at every 30 seconds across Japan. The broken line indicates the epicentral distance of 33° and 40°.

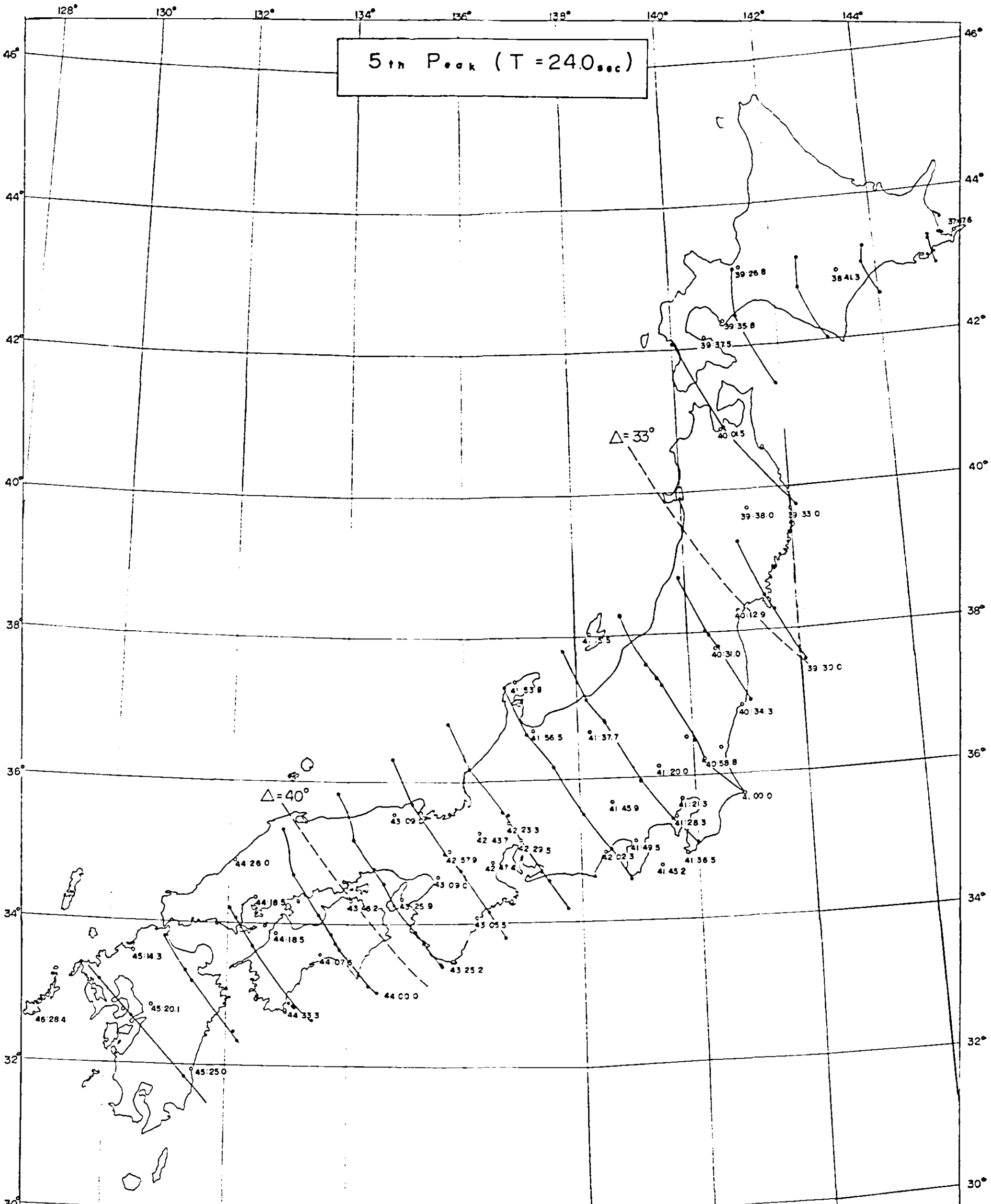

Fig. 6. Wave front of the 5th peak at every 30 seconds across Japan. The broken line indicates the epicentral distance of 33° and 40°.

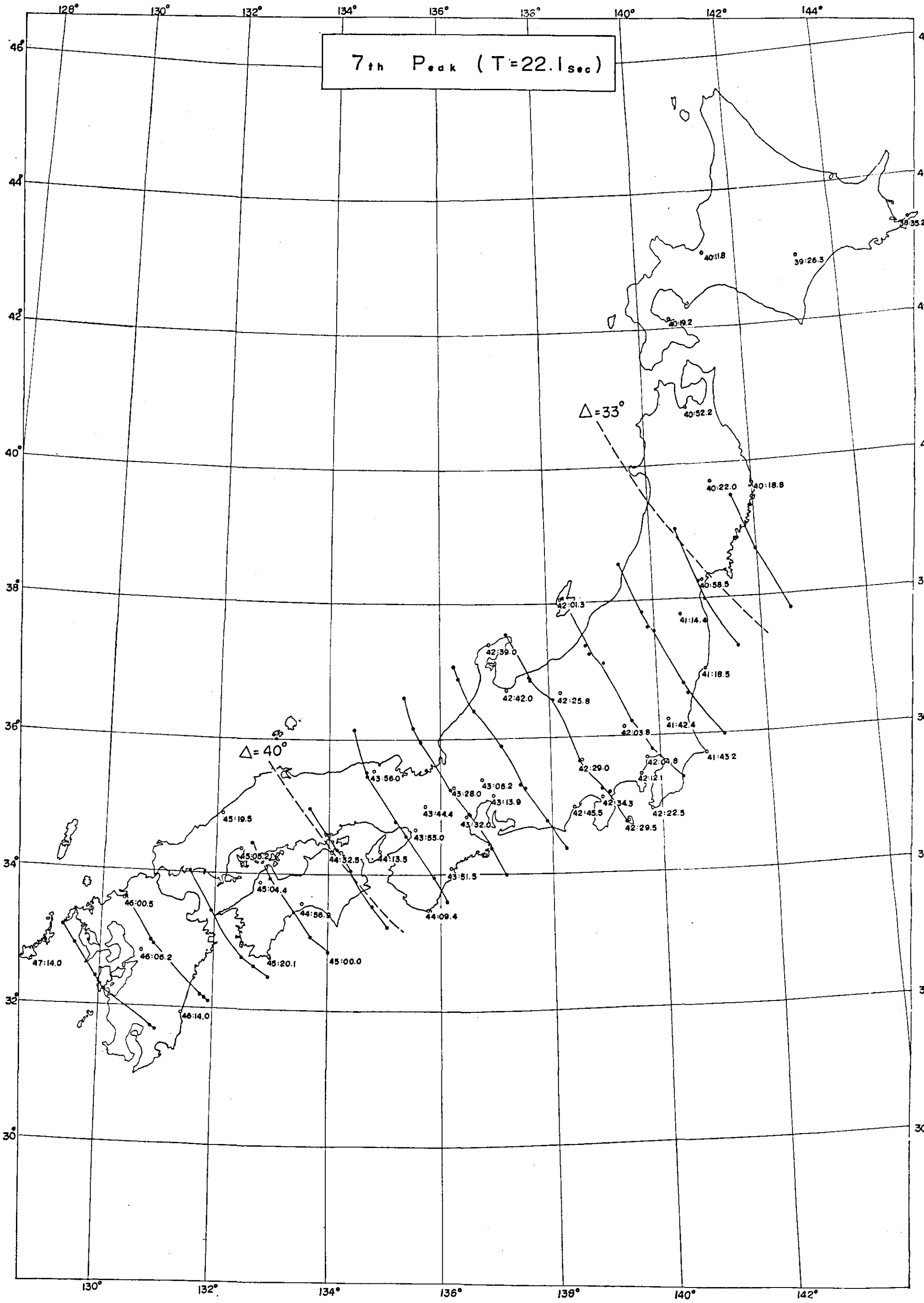

Fig. 7. Wave front of the 7th peak at every 30 seconds across Japan. The broken line indicates the epicentral distance of 33° and 40°.

3. Wave front chart

The arrival times of the 1st, 2nd, 3rd, 5th and 7th peaks are indicated on the map of the stations as shown in Figs. 3, 4, 5, 6 and 7 respectively. The position of the peak for successive increments in travel time of 30 sec is interpolated between stations, and is plotted on the map. Wave fronts are drawn to pass through these interpolated points.

The dashed lines in these figures indicate the epicentral distances of 33° and 40°.

The departure of the wave fronts from the equi-epicentral distance line from the Hokkaido to the Kanto region is caused by difference in the propagation path before the waves arrived at Japan.

Table 3. List of group velocity.

Station	Epicentral distance	Travel time of the 1st peak	Group velocity
Sapporo	3383 km	902.3 sec	3.74 km/sec
Miyako	3543	926.4	3.82
Sendai	3710	964.0	3.85
Kakioka	3899	1008.3	3.86

As shown in Table 3, we observed a lower group velocity for waves arriving at Sapporo than for those at Miyako, Sendai and Kakioka. The latter velocities agree with the velocity from Aleutian to Tsukuba observed by Santō (1960). It may be that the peaks reached at the Hokkaido region have lower velocity, because their propagating path lies mostly in the island region of the Aleutian and the Kurile.

As shown in Figs. 5 and 7, the irregularity of the wave front increases as the wave period becomes shorter. To determine the phase velocity accurately, it is desirable that the wave fronts be straight lines. From this point, the 2nd peak is the best, followed by the 3rd, 1st, 5th and 7th respectively.

A wave front chart may be used in a rough measurment of phase velocity. But, in order to attain a higher accuracy, we applied the least squares method to the data from many stations within a certain area to compute the phase velocity for the area. Our stations are divided into 10 regions as shown in Fig. 8. It is intended that the boundary of regions coincides with that separating major geological

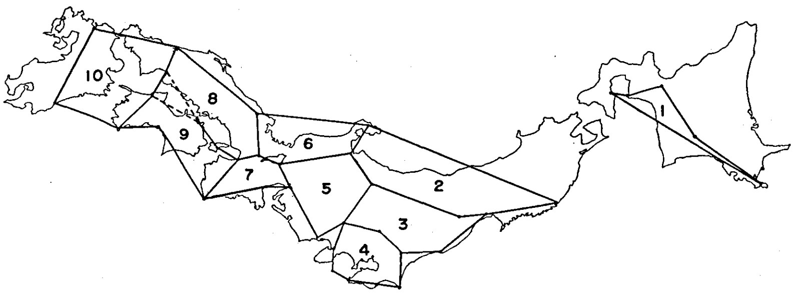

Fig. 8. Division of stations into 10 groups: 1. southern Hokkaido; 2. Shinetsu; 3. northern Kanto; 4. southern Kanto; 5. Chubu; 6. Hokuriku; 7. Kii; 8. Chugoku; 9. Shikoku; 10. Bungo.

provinces in Japan. Care is also taken that the wave front be nealy a straight line within each region.

4. Application of the Least Squares Method

We use the same formula as given in the first paper. The reference point for each region is listed Table 4 together with the epicentral distance and the great circle direction to the epicenter.

Table 4. List of reference points with their epicentral distances and great circle directions to the epicentre.

Station	Region	Epicentral distance		Great circle direction (from north)	
		deg.	min.	deg.	min.
Sapporo	1	30	26	59	27
Aikawa	2	35	11	53	01
Kumagaya	3	35	37	50	50
Yokohama	4	35	54	50	02
Nagoya	5	37	46	51	10
Kyoto	6	38	38	50	04
Osaka	7	39	00	49	44
Hiroshima	8	41	08	49	42
Kochi	9	40	57	48	56
Fukuoka	10	42	56	49	08

Table 5. The values of phase velocity V, direction of propagation θ and crustal thickness obtained under Press' and Aki's standard phase velocity curves and errors in various rigions.

Wave No.	Period	V (km/sec)	θ (rad.)	Crustal thickness	
				Press' model (km)	Aki's model (km)
South Hokkaido					
1	37.0	3.708±0.254	1.2898±0.0985	57±20	39±21
2	29.6	3.652±0.065	1.3971±0.0467	49± 5	35± 5
3	25.8	3.583±0.080	1.5298±0.0339	48± 6	34± 5
5	23.8	3.416±0.051	1.6391±0.0226	56± 4	40+ 3
7	22.0	3.422±0.177	1.1766±0.0659	53±16	35± 8
			average	52± 1	38± 1
Shinetsu					
1	37.2	3.829±0.034	1.1250±0.0113	45± 3	25± 4
2	29.1	3.637±0.080	1.1383±0.0286	50± 6	35± 5
3	25.2	3.593±0.085	1.1398±0.0306	46± 6	32± 5
5	23.2	3.582±0.049	1.0824±0.0172	43± 3	32± 3
7	22.1	3.458±0.984			
			average	45± 1	31± 2
North Kanto					
1	36.3	3.876±0.034	0.9656±0.0089	39± 5	
2	28.2	3.600±0.060	1.0707±0.0166	51± 3	36± 4
3	25.3	3.566±0.083	1.0410±0.0230	48± 6	35± 5
5	23.7	3.530±0.019	1.0293±0.0054	46± 2	33± 4
7	21.6	3.548±0.287	1.1783±0.0802	41±17	30±13
			average	47± 1	34± 1
South Kanto					
1	35.4	3.837±0.050	0.9077±0.0134	43± 6	24± 5
2	28.6	3.755±0.066	0.8608±0.0226	40± 5	26± 5
3	25.9	3.629±0.064	0.8712±0.0233	45± 4	31± 4
5	23.9	3.504±0.086	0.8312±0.0248	51± 6	33± 4
7	21.4	3.334±0.093	0.8063±0.0281	60±10	41± 6
			average	45± 2	31± 2
Chubu					
1	40.1	3.538±0.088	1.0309±0.0252		57± 7
2	29.9	3.668±0.095	0.9833±0.0262	48± 7	33± 7
3	26.7	3.605±0.077	0.9809±0.0217	47± 5	33± 5
5	24.0	3.537±0.121	0.9504±0.0345	47± 9	34± 6
7	21.9	3.616±0.173	1.0099±0.0485	38±10	27± 8
			average	46± 1	36± 3
Hokuriku					
1	38.3	3.857±0.192	0.9832±0.0448	41±23	
2	30.8	3.537±0.102	1.0712±0.0249	59± 7	34± 7
3	26.2	3.456±0.065	1.1050±0.0161	57± 5	33± 4
5	23.7	3.405±0.144	1.0858±0.0364	57±15	41± 8
7	21.9	3.264±0.164	1.1140±0.0424		47±17
			average	57± 3	35± 2

(to be continued)

(continued)

Wave No.	Period	V (km/sec.)	θ (rad.)	Crustal thickness	
				Press' model (km)	Aki's model (km)
Kii					
1	39.0	3.910±0.203	0.8868±0.0505	37±30	
2	30.6	3.718±0.101	1.0061±0.0258	46± 7	31± 9
3	26.7	3.704±0.075	1.0559±0.0190	41± 5	28± 4
5	24.1	3.719±0.104	0.9393±0.0269	36± 6	22± 7
7	21.9	3.540±0.065	1.0230±0.0172	43± 4	31± 3
			average	45± 3	29± 1
Chugoku					
1	41.3	3.784±0.106	0.9254±0.0345	55±13	33±14
2	32.1	3.715±0.056	0.9375±0.0188	49± 4	32± 5
3	27.4	3.764±0.087	1.0136±0.0315	38± 6	22± 7
5	24.8	3.649±0.102	1.1171±0.0435	41± 6	29± 5
7	23.0	3.608±0.154	1.2174±0.0755	42± 7	29± 7
			average	45± 2	29± 1
Shikoku					
1	40.2	3.720±0.134	0.8480±0.0371	58± 7	40±16
2	31.4	3.736±0.038	0.9601±0.0120	46± 3	30± 4
3	26.8	3.639±0.075	0.9938±0.0254	46± 5	32± 5
5	24.4	3.738±0.052	0.9696±0.0168	36± 3	23± 4
7	23.2	3.695±0.066	0.9872±0.0219	36± 4	27± 6
			average	42± 2	28± 2
Bungo					
1	40.8	3.786±0.086	0.7795±0.0220	54±10	33±12
2	32.7	3.823±0.060	0.8365±0.0150	40± 6	21± 9
3	28.2	3.720±0.072	0.9015±0.0179	41± 5	28± 5
5	25.3	3.644±0.170	0.9705±0.0420	42±10	25± 9
7	23.3	3.602±0.314	1.0359±0.0761	41±18	30±15
			average	42± 2	27± 1

The phase velocity of Rayleigh waves and the direction of propagation of the peak measured from the north (east positive) are listed in Table 5 with the probable errors, for various regions.

The period and phase velocity averaged over the whole of Japan except the Hokkaido region are shown in Table 6 for each peak.

As shown in Table 5, the probable errors of the velocities of the 1st, 5th and 7th peak are large. In most regions, the probable errors of velocity of the 2nd and 3rd peak are from 1 to 2%. But the probable error for the 1st peak reached to 5% and those for the 5th and 7th sometimes even larger. For example, at the Bungo region (region 10), the probable errors of velocity for the 1st, 2nd and 3rd peak are less than 3%, but that for the 5th peak is 5% and that for the 7th peak is 9%. These are expected from the irregularity of the wave fronts in the chart as seen in Figs. 3, 6 and 7.

The large error for the 1st peak may be due to the fact that the zero point preceding the peak is not very clearly defined on the record.

Table 6. Phase velocity and crustal thickness in Japan except south Hokkaido.

Wave No.	Period	Phase velocity	Crustal thickness	
			Aki's model	average
1	38.3 sec	3.793 ± 0.037 km/sec	31 ± 5 km	
2	30.3	3.688 ± 0.029	33 ± 3	
3	26.4	3.631 ± 0.031	32 ± 2	31.7 ± 0.4 km
5	24.1	3.590 ± 0.036	31 ± 2	
7	22.1	3.518 ± 0.048	32 ± 2	

The errors for the 5th (period: 24–26 sec) and 7th (period: 21–24 sec) peaks are large, perhaps because these peaks have shorter wave lengths and are more easily subject to lateral refractions due to the complex topography of the shallow crustal structure.

5. Crustal thickness

In determining the crustal thickness from the phase velocity of Rayleigh waves, we used standard phase velocity curves based on Press' model 6EG (1960) and Aki's model 6EJ (1961). The shear velocity distributions of both models are shown in Fig. 9. The standard phase velocity curves based on these models are shown in Fig. 10 and Fig. 11, where the observed average phase velocities in Japan given in Table 6 are also shown.

The thickness of the crust obtained by the application of Press' and Aki's standard curves to the observed phase velocity value is given in Table 5 for various regions.

Four or five values of the thickness of the crust are obtained for each region from different peaks. They are averaged for each region with the weight inversely proportional to the variance as determined by the least squares method.

The weighted average is computed by the formulas.

$$x_0=\frac{\sum_{k=1}^{n}P_k x_k}{\sum_{k=1}^{n}P_k}$$

$$E=C\sqrt{\frac{\sum_{k=1}^{n}P_k\delta_k{}^2}{(n-1)\sum_{k=1}^{n}P_k}}$$

where

$$P_1:\ P_2\cdots\cdots P_n=\frac{1}{e_1^2}:\frac{1}{e_2^2}:\cdots\cdots:\frac{1}{e_n{}^2}$$

x_0: the average thickness of the crust,
x_k: the thickness of the crust obtained from the kth peak,
E_0: the probable error of the thickness,
e_k: the probable error of the thickness obtained from the kth peak,
δ_k: x_k-x_0,
C: 0.766 in case $n=4$,
0.740 in case $n=5$.

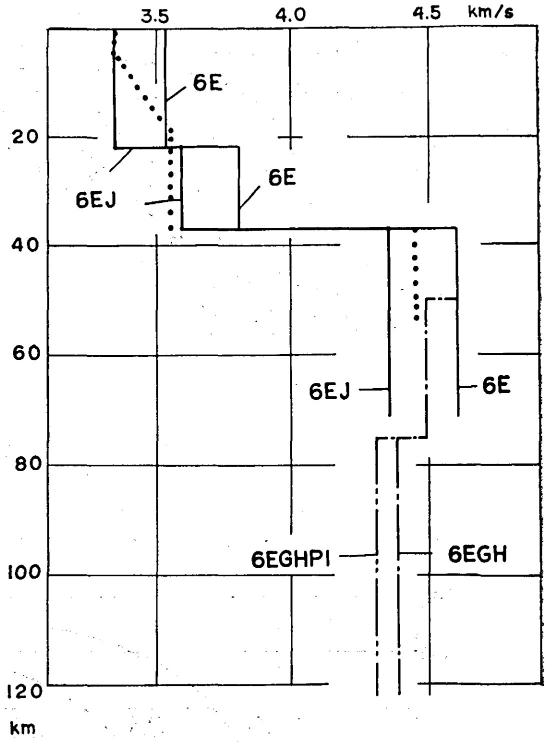

Fig. 9. Shear velocity distribution at depth for various crust-mantle models. 6EG is the model adopted by Press in his construction of standard phase velocity curves. 6EJ is adopted the phase velocity data in Japan.

It is clear from Fig. 10 that the average phase velocity in Japan coincides better with Aki's standard phase velocity curves than with Press'.

Further, the refraction study of the crustal structure in Japan by the explosion-generated seismic waves has been getting to a thickness of from 25 to 35 km in most of the Honshu region. The thickness obtained from Aki's standard phase velocity curves ranges from 27 to 36 km and those obtained from Press' standard phase velocity curves range from 42 to 57 km. It is clear that Aki's model better explains the observation in Japan.

Aki's model was obtained by modifying Press' case 6E (Fig. 9), which is identical with 6EG except that the low velocity layer in the mantle was neglected, in such a way that the velocities in all the layers

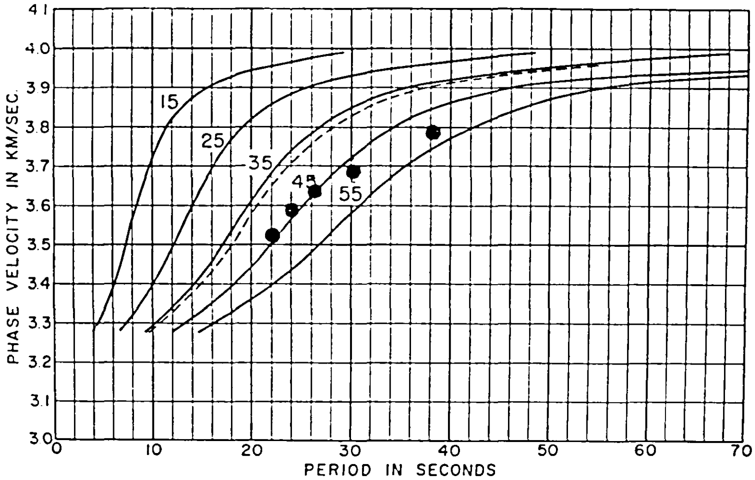

Fig. 10. Press' standard phase velocity curves (Press, 1960). The average phase velocity in Japan (except Hokkaido) are shown.

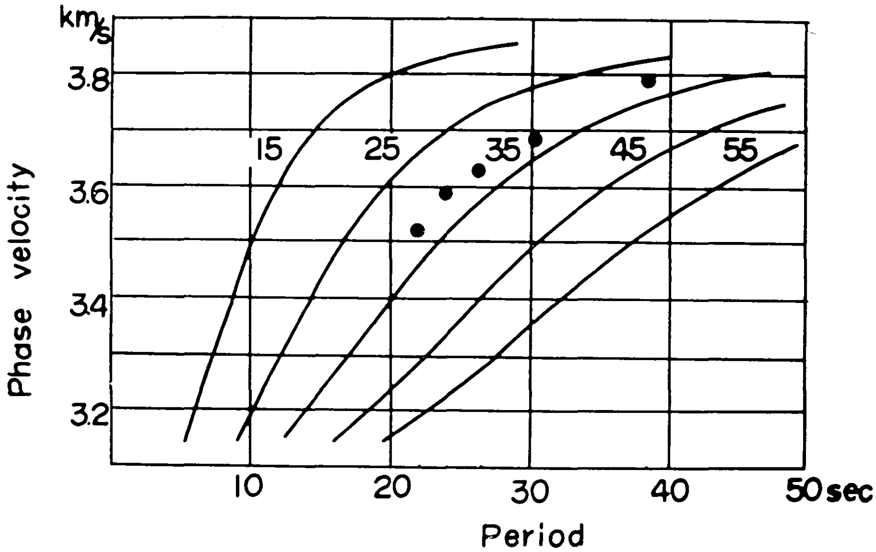

Fig. 11. Aki's standard phase velocity curves (Aki, 1961). The average phase velocity in Japan (except Hokkaido) are shown.

were reduced by 5.5%.

The average thicknesses in each region obtained by the use of Aki's standard phase velocity curves are shown in Fig. 12. The corresponding map obtained in the first paper is reproduced in Fig. 13.

There are 4 regions common to both papers. These regions are as follows:-

Previous result	Present result
S. W. Kanto (38±1 km)	S. Kanto (31±2 km)
	N. Kanto (34±1 km)
Chubu (46±1 km)	Chubu (36±3 km)
Kinki (27±4 km)	Kii (29±1 km)
Seinan (29±3 km)	Shikoku (28±2 km)
	Bungo (27±1 km)

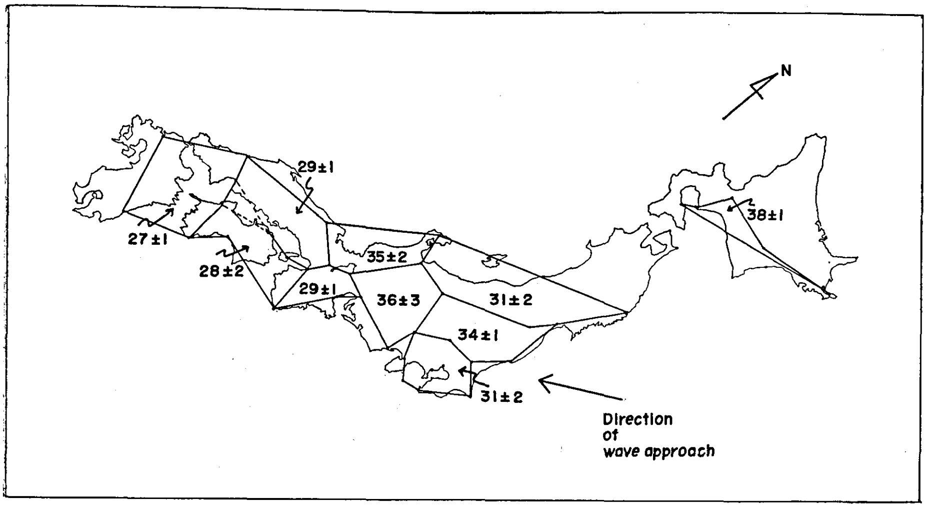

Fig. 12. Crustal thickness for each region obtained by the use of Aki's standard phase velocity curves.

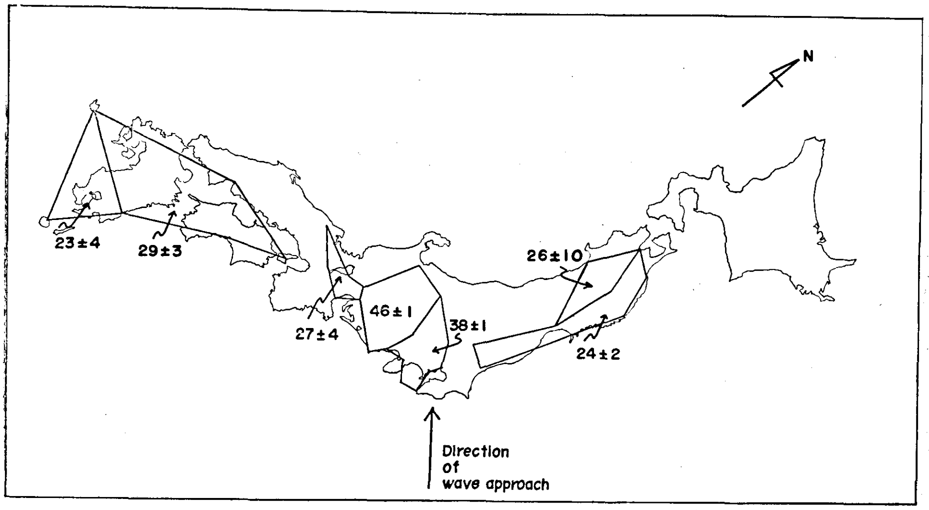

Fig. 13. Crustal thicknese in Japan obtained by the Aki's standard phase velocity curves from the Rayleigh waves of a Samoa shock (Aki, 1961).

The S. W. Kanto region in the first paper does not include a part of the S. Kanto region (Chiba Pref. and a part of Ibaragi Pref.) studied in this paper. The Chubu region covers nearly the same area in both papers.

The thickness in the Kinki and the Seinan region agree with the thickness observed in this paper within a limit of errors, but those in the S. W. Kanto and the Chubu regions show a little difference between each paper. The difference for the Kanto region may be explained by the fact that the area in the present paper was spread out to the Pacific Ocean, and may have a thinner crust, while the area in the previous paper included a part of the Chubu region with a thicker crust.

A map of crustal thickness in Japan is tentatively drawn from the phase velocity of Rayleigh waves as shown in Fig. 14. This map is

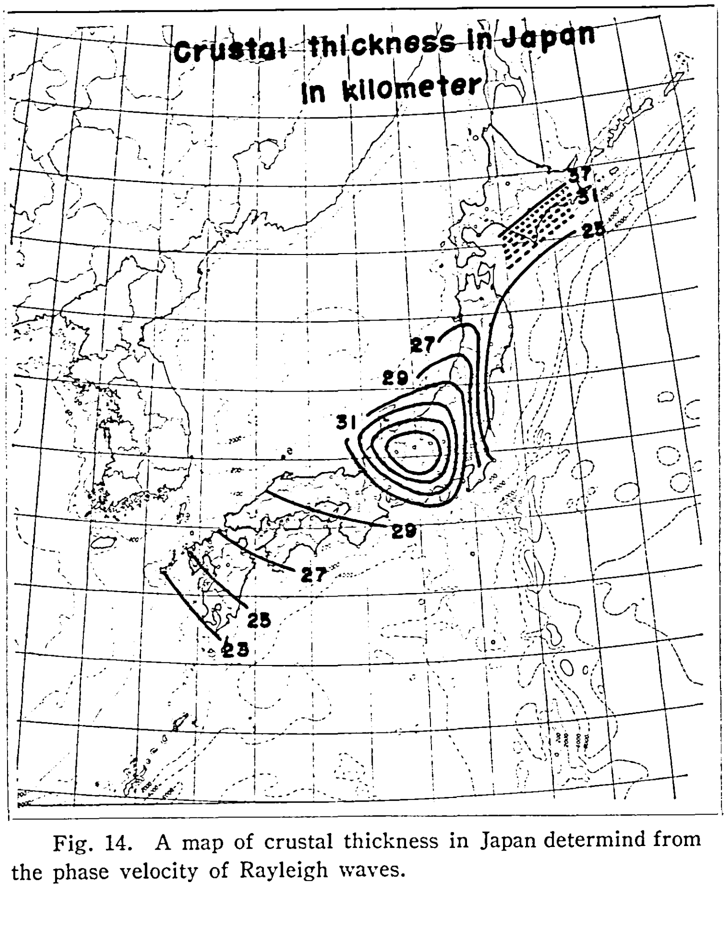

Fig. 14. A map of crustal thickness in Japan determind from the phase velocity of Rayleigh waves.

based on the valued of crustal thickness given in Figs. 12 and 13. The crust in the Hokkaido region seems to be thicker than the crust in the Honshu region. Further study is necessary to establish this.

6. Comparison of the result with those derived from Explosion Seismology

The crustal structure in central Japan was derived from the Miboro Explosion-Seismic Observations by the Research Group for Explosions Seismology (1961). The crustal thickness was measured as 27 to 30 km in one of the solutions in the Kinki region (the refraction profile cuts regions 5, 6, 7, 8 and 9), and as 30 to 38 km in the Chubu and Kanto regions (the refraction profile cuts the regions 2, 3, 4 and 5). The thicknesses of these regions are consistent with the map in Fig. 14 with minor exceptions.

The crustal thickness in the nothern Kanto region (a part of region 2 and 3) was measured as 25 to 30 km from the refraction study (Usami etal., 1958) and as 28 to 33 km from Fig. 14.

The crustal thickness in the eastern part of the Shinetsu region and the northern Kanto region was ascertained as being 20 to 28 km from the refraction study (Matuzawa et al., 1959) and about 25 km in Fig. 14.

As described in the previous paper, the thickness of 20 to 25 km for the Tohoku region agree with the thickness obtained from the refraction study by Matuzawa (1959). Thus, the values of crustal thickness obtained from the refraction study generally agree with those obtained from the phase velocity data.

7. The Bouguer gravity anomaly, the elevation and the phase velocity of Rayleigh waves

We obtained the average Bouger gravity anomaly for each of our regions from the map compiled by Tsuboi (1954), and also the average elevation. These values are listed in Table 7 together with the phase velocity of Rayleigh waves with the period of 30 sec which was obtained from the average crustal thickness in each region by the use of Aki's standard phase velocity curves. The corresponding data for the regions studied in the previous paper is listed in Table 8.

Fig. 15 shows the relation between the phase velocity of Rayleigh waves with the period of 30 sec and the average Bouguer anomaly for

Table 7. The average Bouguer anomaly, the average elevation and the phase velocity of Rayleigh waves with the period of 30 sec.

	Bouguer anomaly	Elevation	Phase velocity (T=30 sec)
S. Hokkaido	47.7 mgal	229 m	3.61 km/sec
Shinetsu	38.8	243	3.72
N. Kanto	34.7	669	3.67
S. Kanto	33.6	173	3.72
Chubu	−26.8	860	3.64
Hokuriku	2.7	231	3.66
Kii	21.5	371	3.73
Chugoku	3.6	217	3.73
Shikoku	20.4	−16	3.74
Bungo	−5.4	133	3.75

Table 8. The average Bouguer anomaly, the average elevation and the phase velocity of Rayleigh waves with the period of 30 sec.

	Bouguer anomaly	Elevation	Phase velocity (T=30 sec)
E. Tohoku	98.7 mgal	283 m	3.77 km/sec
W. Tohoku	56.0	365	3.76
S.W. Kanto	−1.0	553	3.56
Chubu	−23.5	953	3.45
Kinki	−10.3	274	3.75
S. W. Japan	1.4	158	3.72

various regions in Japan and the United States. The data for the United States is obtained by Ewing and Press (1959). It is interesting to note that the points for the regions to the east of the Fossa Magna (open circle), those for the region to the west (closed circle) and those for the United States are separated on this diagram. This fact may have an important bearing on the apparent difference between east Japan and west Japan in geology and geotechtonics.

In the Bungo region, the crustal thickness is normal despite the presence of the negative Bouguer anomaly.

The relation between the crustal thickness and the elevation for various regions in Japan is shown in Fig. 16. The theoretical relation

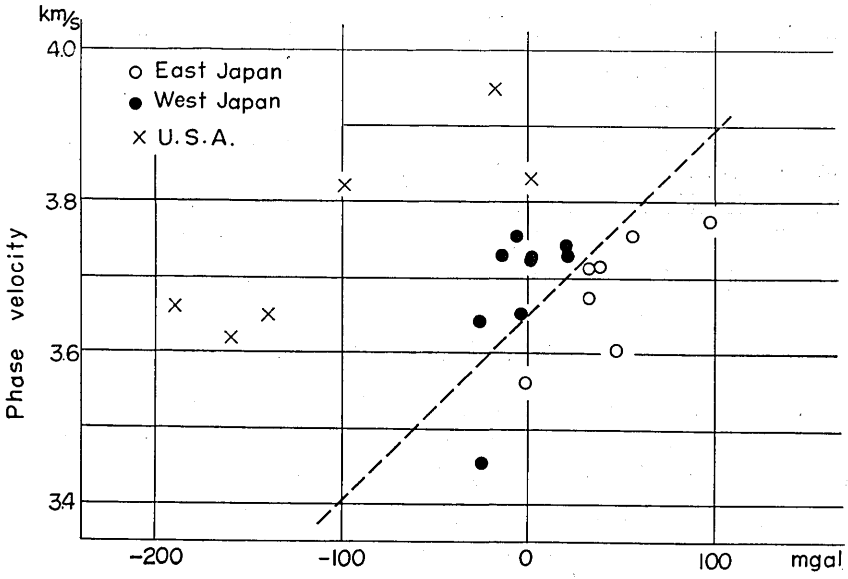

Fig. 15. Relation between phase velocity of Rayleigh waves with the periods of 30 sec and the average Bouguer anomaly for various region in Japan and the United States. The data for the United States are obtained by Ewing and Press (1959).

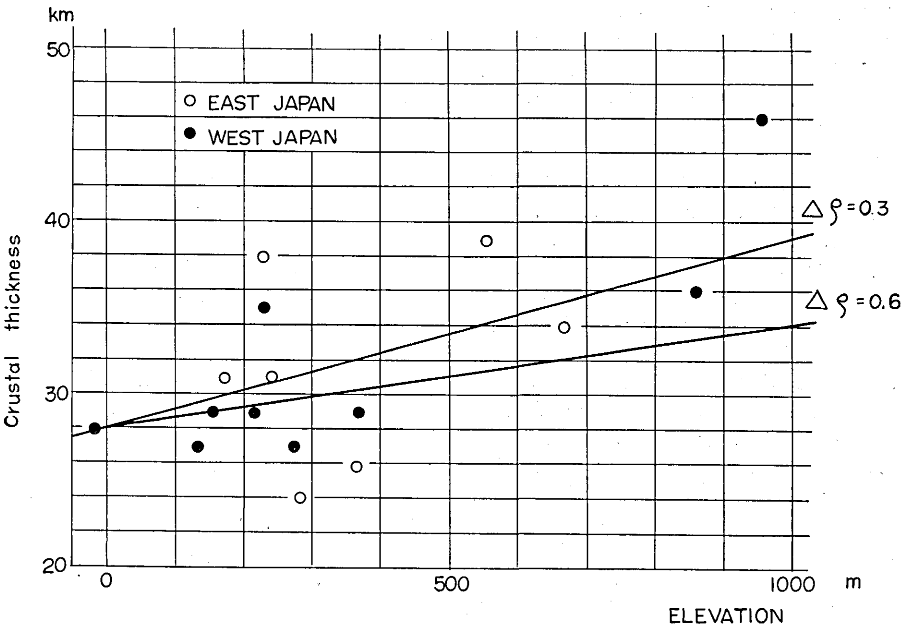

Fig. 16. Relation between the crustal thickness and the elevation for various regions in Japan.

based on the assumption of Airy's isostacy is also shown for the cases where the density contrast $\Delta\rho$ between the mantle and the crust are 0.3 and 0.6 gr/cm^3. The crustal thickness at sea level is assumed as 28 km. The points in this figure, although quite diverged, seem to favour the value 0.3 gr/cm^3 as the density contrast.

The Hokkaido region seems to be different from other regions as seen in Figs. 15 and 16. More detailed study of this region is necessary to draw further conclutions.

8. Acknowledgement

The writers' thanks are extended to all the seismologists at the stations of the Japan Meteorological Agency for their cooperation in making their records available to them. The writers' thanks are also due to Professors Takahiro Hagiware and Hirokichi Honda, Assistant Professors Toshi Asada and Setumi Miyamura, and members of Hagiwara, Honda, and Miyamura laboratories.

References

Aki, K., Crustal Structure in Japan from the Phase Velocity of Rayleigh Waves, Part 1: Use of the network of seismological stations operated by the Japan Meteolo-gical Agency, *Bull. Earthq. Res. Inst.*, **39**, (1961), 249-277.

Matuzawa, T., Matumoto, T. and Asano, S., On the Crustal Structure Derived from Observations of the Second Hokoda Explosion, *Bull. Earthq. Res. Inst.*, **37**, (1959), 509-524.

Matuzawa, T. On the Crustal Structure in North-East Japan by Explosion Seismic Observations, *Bull. Earthq. Res. Inst.*, **37**, (1959), 123-154.

Press, F., Determination of crustal structure from phase velocity of Rayleigh waves,
Part 1: Southern California, *Bull. Geol. Soc. Am.*, **67**, (1956), 1647-1658.
Part 2: San Francisco Bay Region, *Bull. Seis. Soc. Am.*, **47**, (1957), 87-88.

Press, F., Crustal Structure in California-Nevada Region, *J. Geophys. Res.*, **65**, (1960), 1039-1051.

Santô, T. A., Observation of Surface Waves by Columbia-type Seismograph Installed at Tsukuba Station, Japan. (Part 1) Rayleigh Wave Dispersion across the Oceanic Basin, *Bull. Earthq. Res. Inst.*, 38, (1960), 219-240.

The Research Group for Explosion Seismology, Crustal Structure in Central Japan as Derived from the Miboro Explosion-Seismic Observations, Part 1. Explosion and Seismic Observations, *Bull. Earthq. Res. Inst.*, **39**, (1961), 285-326.

The Research Group for Explosion Seismology, Crustal Structure in North Kwantō District by Explosion-Seismic Observations. Part 1. Description of Explosion and Observations, *Bull. Earthq. Res. Inst.*, **36**, (1958), 329-348.

Tsuboi, C., Gravity Survey along the lines of precise levels throughout Japan by means of Worden gravimeter, Part 4. Map of Bouguer anomaly distribution in Japan based on approximately 4,500 measurements, *Bvll. Earthq. Res. Inst.*, Suppl. 4 (1954), Part 3.

Usami, T., Mikumo, T., Shima, E., Tamaki, I., Asano, S., Asada, T., and Matuzawa T., Crustal Structure in North Kwantō District by Explosion-Seismic Observations, Part II, *Bull. Earthq. Res. Inst.*, **36**, (1958), 349-357.

---

14. レーリー波位相速度法による日本の地下構造の研究 (第2報)

東京大学大学院
地球物理専門課程 神 沼 克 伊
地 震 研 究 所 安 芸 敬 一

1957年3月9日のアリューシャンの地震による，レーリー波 (周期20秒～40秒) は，気象庁ウィーヘルト観測網により，かなりよく記録された (第1図). 気象庁の御好意により集められた記録のうち45カ所の記録を解析して，日本各地でのレーリー波位相速度が求められた. 位相速度の測定には，最小自乗法を応用した.

本報では，前報で取扱うことのできなかつた地域，特に北海道，北陸，紀伊などを取扱うことができ (第8図)，前報も含めると，北海道の北部を除いて日本列島全体についての位相速度が求められた.

主な結果は次の通りである.

1. 同一地域について，本報と前報の結果は大体一致した. 西日本では，その一致は完全であるが，中部地方では，波が日本列島に直角に入る方が，多少速度が遅くなるようであるが，これは今後の研究が必要である (第12, 13図).
2. 二回の結果を用いて，位相速度法により求めた日本のモホ等深線をひいてみた (第14図).
3. この等深線と重力のブーゲー異常とは，非常によく似た傾向を示している.
4. 今まで得られている爆破から求めた地殻の厚さとも，関東地方の一部や関西地方の一部を除くと，大体よく一致する.
5. 位相速度と重力のブーゲー異常との関係を図にすると (第15図)，フォッサマグナの東と西は，その図上ではつきりと分離する.